TECHNISCHE UNIVERSITÄT WIEN
Vienna | Austria

**Master Thesis**

# Evaluation and testing of a self-filling particle trapping microfluidic chip

carried out for the purpose of obtaining the degree of Master of Science (MSc or Dipl.-Ing. or DI)

submitted at TU Wien, Faculty of Physics, Master programme Biomedical Engineering

**Nemanja Dimitrijevic**

Mat.Nr.: 01641956

under the supervision of

Univ.Prof. Dipl.-Ing. Dr.techn. Gerhard Schütz

Institute of Biophysics

Co-supervision

Christoph Trenzinger, MSc

Vienna, February 2023

*Affidavit*

I declare in lieu of oath, that I wrote this thesis and performed the associated research myself, using only literature cited in this volume. If text passages from sources are used literally, they are marked as such.

I confirm that this work is original and has not been submitted elsewhere for any examination, nor is it currently under consideration for a thesis elsewhere.

I acknowledge that the submitted work will be checked electronically-technically using suitable and state-of-the-art means (plagiarism detection software). On the one hand, this ensures that the submitted work was prepared according to the high-quality standards within the applicable rules to ensure good scientific practice "Code of Conduct" at the TU Wien. On the other hand, a comparison with other student theses avoids violations of my personal copyright.

Vienna, 12.02.2023

*City and Date*

*Signature*

# Acknowledgements

I would like to express my sincerest gratitude to the Biophysics Research Unit which supported me in every possible way with their friendship and expertise during the course of this work.

Furthermore, I would like to thank Mario Brameshuber, who was a great help with his positive manner and helpful tips and who gave me the opportunity to work on this project in the first place.

I would especially like to thank my supervisor Christoph Trenzinger for his constant support, purposeful advice, and friendship during the course of the master's thesis. Without his design for the SELTRAP chip this project would not have been possible.

Lastly, I would like to express a big thank you to my fiancée Maja, without her constant support and devotion this work would not have been possible.

# Abstract

The ability to trap single cells inside a microfluidic chip and subsequent imaging is normally paired with the use of a precise and expensive external pressure source to control the liquid flow. Here we present a self-filling particle trapping chip, which can be used without additional equipment. Different designs of hydrodynamic cell traps were evaluated using cell sized beads and Jurkat T cells. Also, how different plasma treatment conditions of the PDMS surface combined with accelerated aging influence the trapping ability of the chips was investigated. The cell-trapping and self-filling function of the chip could be validated but optimisations of the design are recommended to increase the efficiency.

# Contents

# 1. Introduction

## 1.1. Project goals

The aim of this master thesis is to validate and test a self-filling particle trapping chip (SELTRAP) which was designed for single cell microscopy and with focus on user-friendly handling procedure and low production costs compared to other designs. Different designs of this microfluidic chip were envisioned, and the goal is to find out which of these designs offers the best trapping efficiency and how different chip conditioning parameters influence this efficiency. To fulfil this goal, methods for production, conditioning and handling are being developed. Furthermore, cell-sized beads and different types of cells are used to test the particle trapping properties of these chips. Also, a low-cost water contact angle measurement device is introduced to measure the surface energy of plasma treated PDMS and to be able to estimate the bonding behaviour to glass.

## 1.2. Microfluidics

### 1.2.1. Definition

The term microfluidics refers to systems that can move fluids in the micro- to nanolitre range with channel sizes ranging from less than one to up to 100 µm. Applications of microfluidics range from lab-on-a-chip (LOC), bio-microelectromechanical systems (BioMEMS) or miniaturised total analysis systems (µTAS). Microfluidics as a tool help in areas of drug development, protein crystallisation, organ-on-a-chip and many more. A key characteristic of microfluidics is laminar flow, which is typically expressed by low Reynolds numbers (see Eq. I) (<<1).Within a microfluidic channel network, viscous drag dominates over inertia forces and mass transport is mostly driven by diffusion. [1–3]

$$Re = \frac{\rho * v * d}{\eta} \quad (I)$$

ρ = density [kg/m$^3$]
v = flow speed [m/s]
η = dynamic viscosity of the fluid [N*s/m$^2$]
d = diameter of the channel [m]

Microfluidic applications have a very large impact in the field of biology and medicine due to their offered advantages: small volumes, low cost, high throughput, and short reaction time.

The technology is used to scale down conventional equipment and technology and its applications in these fields range from cell and nucleic acid analysis up to protein engineering and high-throughput screening. [4]

### 1.2.2. Soft Lithography

Soft Lithography is a technique used to replicate nano- and microscale structures for microfluidic chip production. The most commonly used material for microfluidic systems in research is PDMS (Polydimethylsiloxane ($(CH_3)_2SiO)_n$) which offers a variety of important properties for these. Apart from the easy combination with glass systems and its ability to replicate even nanometer-sized structures its other key properties such as transparency, biocompatibility, low autofluorescence as well as its gas permeability play important roles. But PDMS also has its downsides which include molecule absorption, swelling in many solvents and its strong hydrophobicity. However, the last point mentioned can be remedied temporarily by exposure to plasma. During plasma treatment of the PDMS surface, polar SiOH groups (which make the surface hydrophilic) are generated on the surface, which can condense with other silanol groups on another surface when brought in close contact. The thereby formed covalent Si-O-Si bonds are the reason why PDMS can be permanently bonded to glass which was also plasma treated to expose its silanol groups (Figure 1). [5,6]

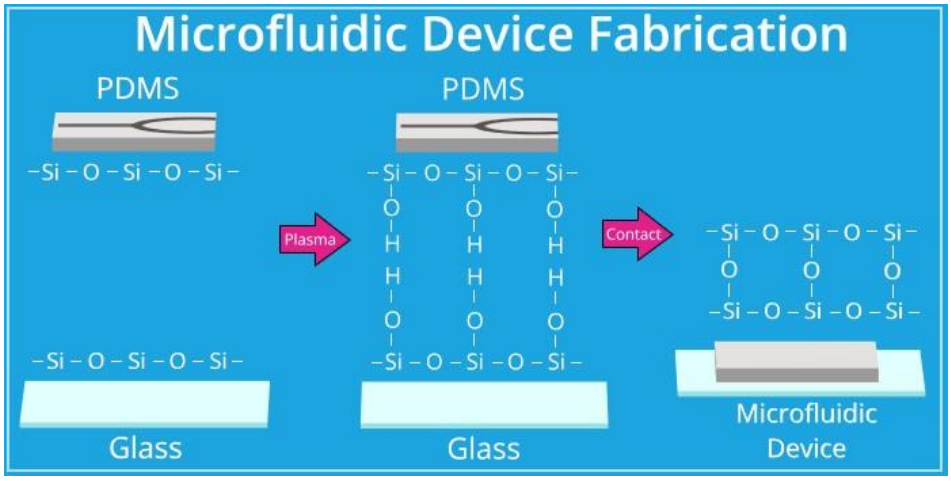


*Figure 1 Chemical reaction of PDMS and glass bonding through plasma treatment of the surfaces. Figure was adapted from the Harrick Plasma web page. [7]*

While PDMS is mostly used in research laboratories for prototyping small-scale production, the microfluidic industry mainly uses thermoplastics (such as COC, COP, PC, PS, PET, PMMA and PVC), which are fit for mass production and are mainly fabricated by injection moulding

or hot embossing. Next to the thermoplastic polymers, paper plays an important role in commercially disposable bioassays. [8]

### 1.2.3. Microfluidics in single cell analysis

Conventionally used assays for cell analysis measure the average response of a whole population of cells, with the assumption that this is also representative for a typical cell in the population. However, individual cells may behave quite differently from each other. This cellular heterogeneity within a population often arises through genetic drifts. Microfluidics can be used to circumvent this problem of whole population testing by enabling the analysis of single cells. There are different concepts for single cell trapping with microfluidics which can either be a hydrodynamic trapping technique, like the LOC concept introduced in this master´s thesis, but can also include dielectrophoretic, magnetic or acoustic systems. [9,10]

## 1.3.SELTRAP chip

SELTRAP stands for self-filling particle trapping chip and is a Lab-on-a-chip concept with the idea and design made by Christoph Trenzinger, MSc. It combines features for particle trapping and self-driven flow on a device which fits on a microscope glass slide (Figure 2).

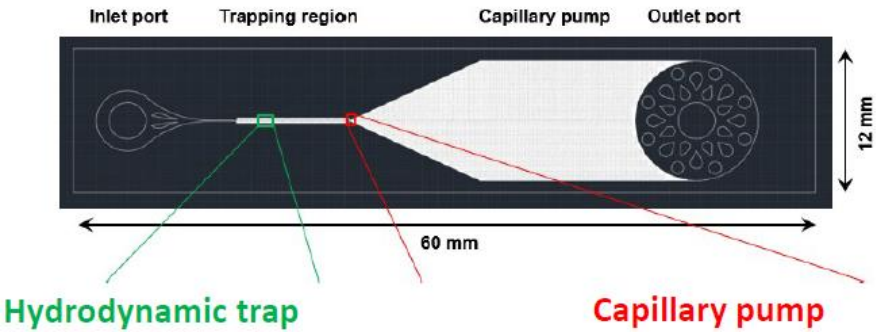


*Figure 2 CAD-Design of the SELTRAP chip. From left to right the different regions, namely inlet port, trapping region, capillary pump, and the outlet port are depicted.*

### 1.3.1. Hydrodynamic trap – Concept

The underlying principle of this self-filling particle trapping chip is a hydrodynamic trap design which is a branched channel with two paths, the trapping, and the flow channel. The design of the system is such that when the trap is not filled with an object, the trapping channel has a lower flow resistance than the flow channel (Figure 3). If the chip is loaded with a particle

suspension the particles will be guided preferentially into the trapping channel. Upon trapping a particle, flow resistance is increased along the trapping channel and the suspension is redirected to the flow channel and a subsequent object will bypass the filled trap.

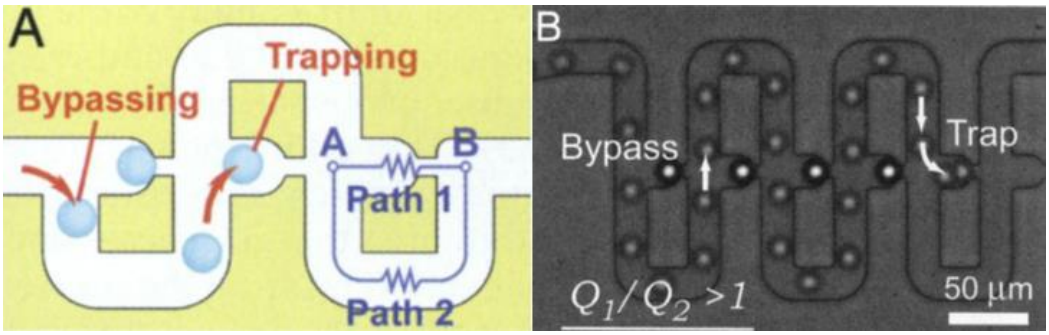


*Figure 3 Left: Schematic visualization of the hydrodynamic trap concept. Right: Simulation of how a particle bypasses already occupied traps. Pictures taken from[11].*

The successful trapping of objects depends on two design criteria, (i) the flow resistance of the flow channel (Path 2) need always to be larger than the flow resistance in the trapping channel (Path 1), and the ratio of the volumetric flow rates Q (Trapping channel Q1 / Flow channel Q2, see Eq. II) must be greater than 3 to guarantee an effective trapping (trapping also occurs at a lower ratio but the probability is lower). [11]

$$\frac{Q_1}{Q_2} = \frac{C_2(\beta_2)}{C_1(\beta_1)} * \frac{L_2}{L_1} * \left(\frac{P_2}{P_1}\right)^2 * \left(\frac{A_1}{A_2}\right)^3 \geq 3 \quad \text{(II)}$$

Q = volumetric flow rates
A = cross section area of the channel
P = channel perimeter
L = channel length
C = laminar friction constant

### 1.3.2. Hydrodynamic trap – Design

Four different designs of dynamic traps were manufactured and tested. The first design 1.0-200 (the last part of the nomenclature depicts the number of traps in series) was copied from the paper by Kimmerling et al. (2016) and the following designs are modified versions of the first one.

1.1-200 has the same number of traps but in contrast to the 1.0-200 version the traps are aligned on the same height which enables easier imaging. Results from the flow simulation (Figure 4) show that at a given mean flow rate of 100µm/s design 1.0-200 shows higher

maximal flow rates through the traps compared to design 1.1. This is expected, as in Design 1.1-200 the exit of one trap is much closer to the entrance into the next one. Hence the total channel length is reduced, which results in lower flow resistance and therefore a lower flow rate.

1.11s-50 has longer trapping and bypassing channels (scaled together to ensure that the volumetric flow rate ratio stays the same as in Design 1.0-200) for potentially better trapping but with a reduced number of 50 traps to ensure that the total flow resistance of the hydrodynamic trapping region stays low.

The last design 1.2s-80 shares similar characteristics to the 1.11s-50 chip with longer channels and fewer traps than the original design but has in contrast rounded trapping channels. Simulations (Figure 4) showed that the flow rate in the unoccupied trapping channels in designs 1.11s-50 and 1.2s-80 is again similar to the original design 1.0. Hence, those designs should allow for easier trapping and fixation of particles inside the traps compared to design 1.1-200, given they are exposed to the same mean flow rate. These simple flow simulations were conducted to prove the functionality of the hydrodynamic trap designs at an estimated mean flow rate and independently of the other features on the SELTRAP chip. Hence, proving the functionality and efficiency of the traps within the microdevice was not part of the simulations.

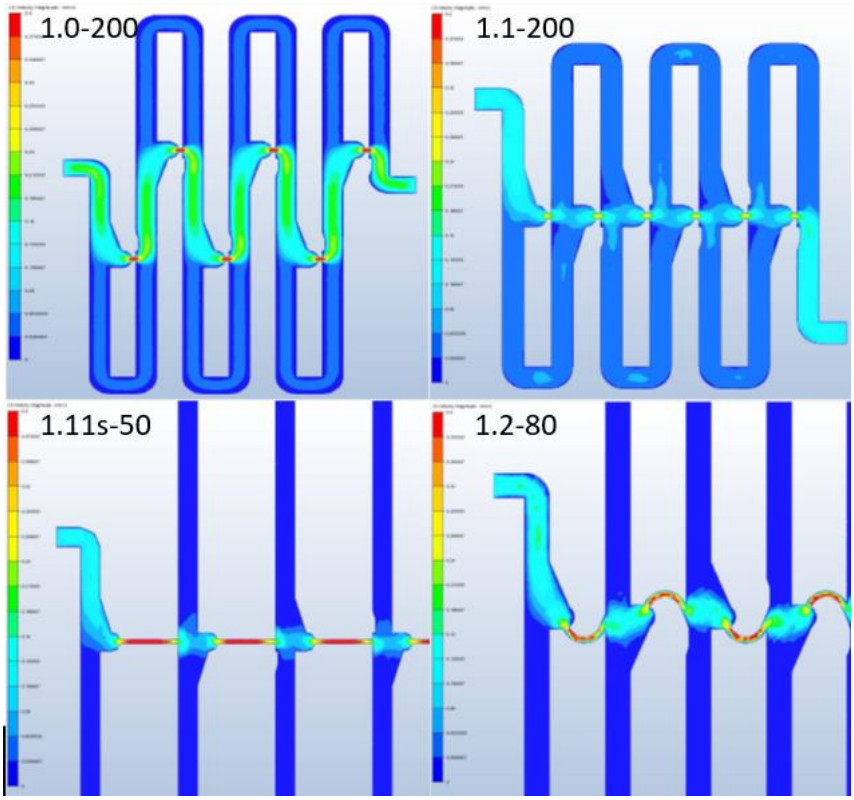


*Figure 4 Flow simulations of different hydrodynamic trap designs showing flow velocities in the channel centers (Color bar: 0-400µm/s). Simulations were conducted by Christoph Trenzinger MSc, using SolidWorks Flow Simulation. Boundary conditions were chosen according to Kimmerling et al. [12] (Mean flow rate 100µm/s)*

The flow channel width in every design is 20 µm, the height 17 µm and the narrowest width of the trapping channel is 5 µm (Design differences can be seen in Figure 5). Thus, in theory every particle larger than 5 µm should be trapped and therefore block the trapping channel.

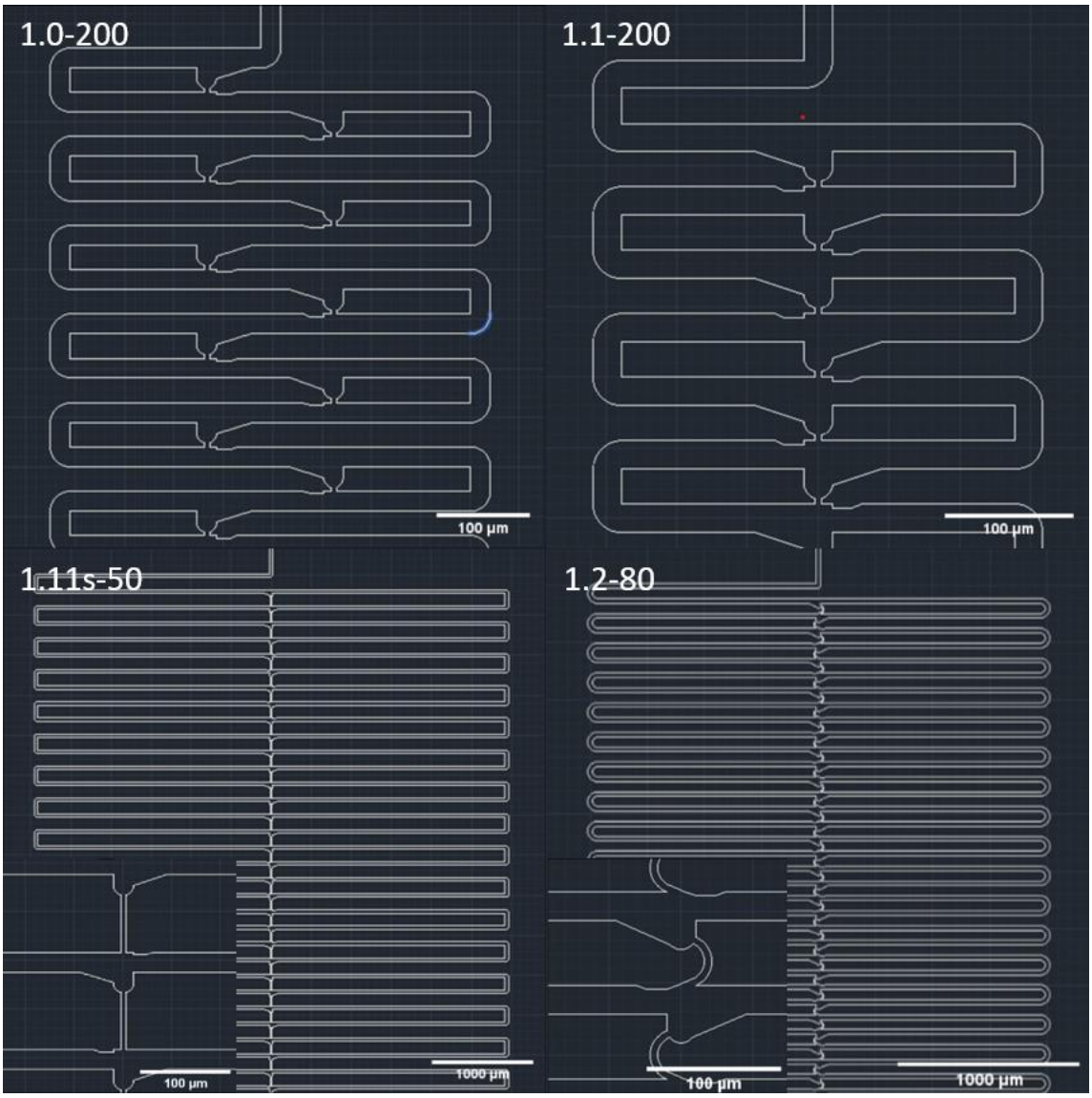


*Figure 5 CAD pictures of the different chip designs. The enlarged cut-outs in the lower left corner of the 1.11s-50 and 1.2-80 designs show the layout of these traps.*

### 1.3.3. Capillary Pump – Concept and Design

To fabricate passively filling microfluidic chips a capillary pump is placed at the end of the microfluidic channel, which exerts the highest capillary pressure in the system and generates a smooth flow of liquid. The liquid displacement inside is facilitated by the principle of capillarity and the surface of the channel is wetted driven by the surface energy of the liquid. This effect can be used to design a microchannel network that takes up the liquid in a specific manner.

The capillary pressure $p_c$ (see Eq. III) depends on three parameters, the channel size (a,b), the contact angle (described in 1.4) between the liquid and the channels top, bottom, left and right wall ($\alpha_{t,b,l,r}$) and the fluid surface tension (γ).

$$p_c = -\gamma * \left(\frac{\cos\alpha_t + \cos\alpha_b}{a} + \frac{\cos\alpha_l + \cos\alpha_r}{b}\right) \text{(III)}$$

There are various design options for a capillary pump, the simplest being just a microchannel with a large enough volume to contain the displaced fluid, or a cavity with integrated support posts for stabilisation. Drawback of this simple designs is the large total flow resistance which occurs if the channels are too long. To get around this problem, a cleverer design must be used, namely placing microstructures such as hexagons or lines at regular intervals inside. This reduces the flow resistance due to the high number of parallel flow paths and is used when higher liquid volumes need to be displaced. [13]

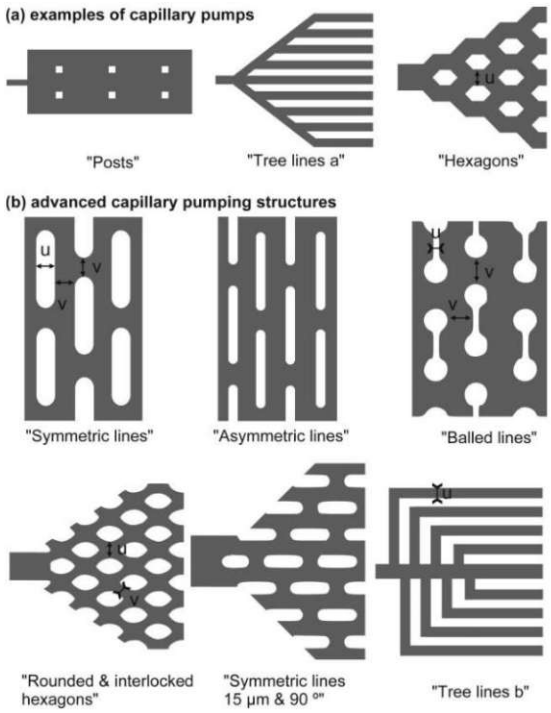


*Figure 6 (a) Examples of simple capillary pump designs. (b) More advanced designs with lower flow resistance compared to simple ones. For the capillary pump design of the SELTRAP-chip the "symmetric lines" design was used. Pictures taken from [13].*

The capillary pump design chosen for the SELTRAP chip ("symmetric lines" depicted in Figure 6) can pump up to 1.0 µl of liquid in about 20 minutes and the total volume it is able to take

up is about 1.7 µl. The elongated pillars (design can be seen in Figure 7, colours of the pillars are inverted in Figure 7 compared to Figure 6) are placed horizontally to receive a filling front that moves into the cone shaped capillary pump without entrapping air.

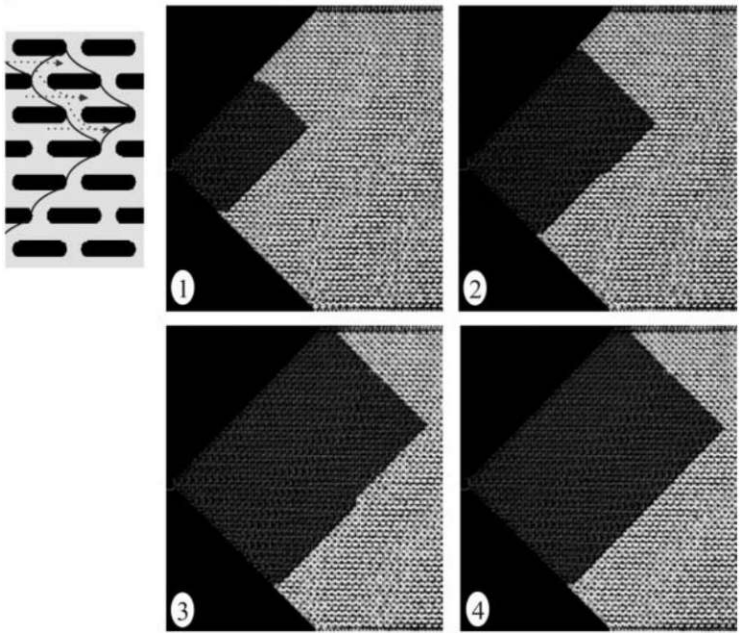


*Figure 7 Right: Horizontally placed pillars displace the liquid into the cone shaped capillary pump without entrapping air. Left: Movement of the filling front depicted. Picture taken from* [13]

To avoid clogging, the distances between the pillars have to be bigger than the target particle / cell sizes which are planned to be used (Mouse $CD4^+$ T-cells have an average size of about 7 µm) but as low as possible to reach the maximum capillary pressure (u, v, w = 12 µm, x = 90 µm, see Figure 8). Moreover, the contact angles need to be low to reach high capillary pressure.

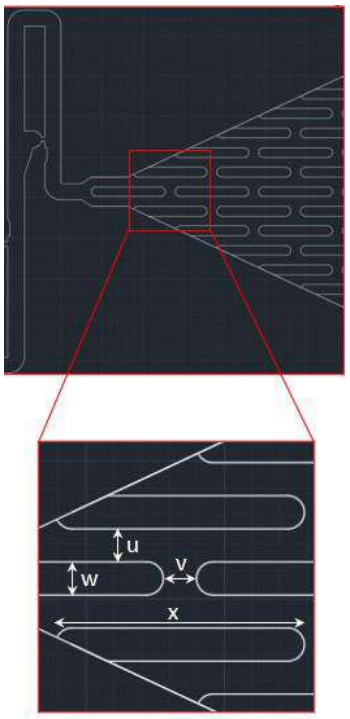


*Figure 8 CAD images of the used capillary pump design for the SELTRAP chip with the measurements of the pillars (u, v, w = 12 µm, x = 90 µm).*

## 1.4. Contact angle

The contact angle between a drop of fluid and a solid surface depends on the surface energy of the surface. PDMS for example has a quite low surface energy and has hence a hydrophobic character. This hydrophobicity, which is unwanted for the self-filling function of the SELTRAP chip, can be modified by plasma treatment of the surface which enlarges its surface energy. During this process, Silanol groups (-OH) develop on the surface of the polymer and due to their polar nature the PDMS surface becomes hydrophilic which is essential for the self-filling of the chip and the bonding to glass. [5]

The surface energy cannot be measured directly but it can be estimated by measuring the contact angle between the PDMS surface and water. The higher the contact angle between the two phases, the lower the surface energy (Figure 9).

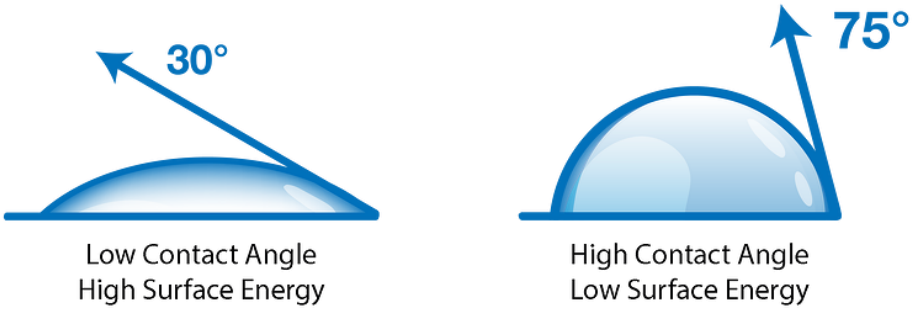


*Figure 9 Difference in contact angle between a liquid drop and a solid surface. Higher surface energy leads to lower contact angle and thus more wettability of a surface due to more surface which is covered by the same volume. Picture taken from [14].*

# 2. Material & Methods

## 2.1. Chip-production

To produce the PDMS (Polydimethylsiloxane) Nanowell chip, Sylgard® 184 Silicone Elastomer kit was mixed in a 10:1 ratio and then placed in a desiccator under vacuum to remove entrapped air bubbles. The mixture was then poured onto a SU8 master, which was produced from a 4-inch silicon wafer using standard photo lithography techniques (SU-8 2015, micro resist technology). The master featured duplicates of the 1.0, 1.1, 1.11s and 1.2 designs (seen in the inner circle in Figure 10). The PDMS was then cured at 70°C for 120 minutes (± 10 min.) to produce a 3 to 4 mm thick PDMS layer. After cooling to room temperature, the inner circle of the casted PDMS (design within the smaller circle in Figure 10) was cut and demoulded. The different chips were then singularized, and the inlet and outlet port were made with a 5 mm biopsy puncher. The prepared chips were then stored, until their usage, in ultra-pure $H_2O$ to keep them dust free.

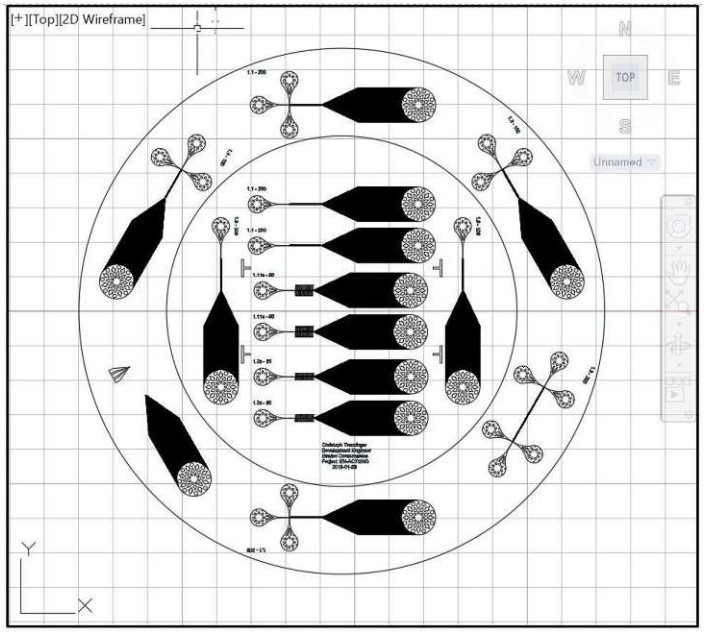


*Figure 10 CAD picture of the used SU8 silicone master. The used chip designs are located inside of the smaller circle as duplicated, while the designs on the outer ring were not intended for usage.*

The pre-cleaning of the glass slide was done by putting them in an ultrasound bath together with a Hellmanex® solution (2% in deionized water) for 30 minutes, followed by rinsing with distilled water three times, drying at 70°C before storing them in glass chambers for usage.

The casted PDMS pieces were dried using a $N_2$ stream and then bonded with a cleaned glass microscope slide after plasma activation (Harrick Plasma, Plasma cleaner pdc-002-ce). The glass slide was plasma-treated for at least 10 minutes and the PDMS chip was activated for 1 to 3 minutes in the plasma cleaner. The glass and the PDMS were treated with a plasma power output of 29,6 W. After the plasma treatment the PDMS chip was placed on the glass slide and the bonding was carried out by applying pressure on the top side of the chip (effective binding was tested by carefully trying to scrap off the PDMS, if this was not possible it was assumed that the binding was successful).

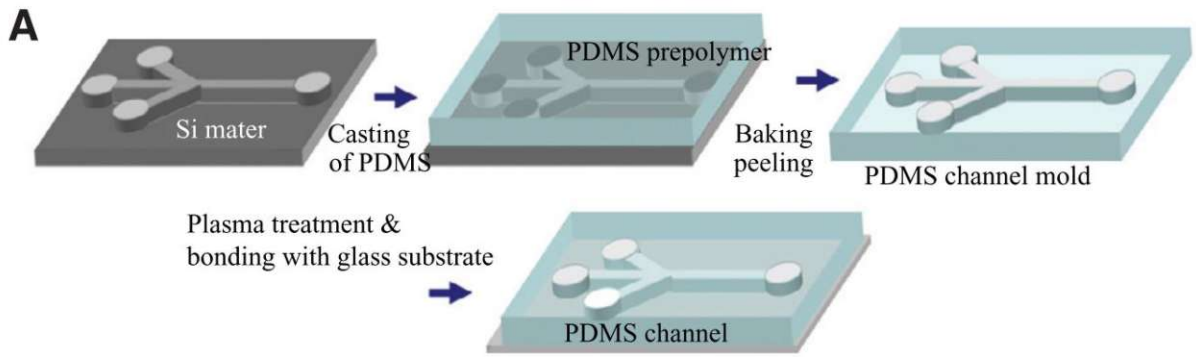


*Figure 11 Schematic representation of microfluidic channel fabrication.* [15]

## 2.2.Cell culture

### 2.2.1. Murine T-cell cultivation

The mouse $CD4^+$ were isolated from the spleen and lymph nodes and the organs were afterwards squashed through a cell sieve (Greiner Bio-One, 70µm, Art-Num: 542070) after extraction, washed with T-cell medium and the spleen cells were additionally treated with a red blood cell lysis buffer. MCC (Moth cytochrome C) peptide with a concentration of 2 mM was added for T-cell selection and the cells were then incubated (37°C and 5% $CO_2$) in 24-well plates with a conc. of $7.5x10^6$ cells/well. After 24h Interleucin-2 (IL-2 eBioscience) with a conc. of 50 U/ml was added. The cells were then split in a 1:1 ratio 48 & 96 hours after isolation. The last step of the cultivation was a density gradient centrifugation with Histopaque®-1119 (by Sigma-Aldrich). The T-cells aggregated after the centrifugation at the Histopaque / T-cell medium interface which could then be carefully removed, and the cells were then seeded again into 24-well plated with a density of $10^6$ cells/ml. The cells could then be used for experiments up to 3 days.

### 2.2.2. Jurkat T cell cultivation

The Jurkat T cells (Jurkat E6.1 wild type) were cultivated in RPMI 1640 with L-Glutamine and 10% FCS at 37°C with 5% $CO_2$ and split two times a week.

### 2.2.3. Cell preparation for SELTRAP chip filling

Both used cell types (murine T-cells and Jurkat T cells) were prepared for the experiments by first centrifuging them for 3 minutes at 350G. The supernatant was then removed, and the cells were resuspended in the same volume of Imaging buffer (50 ml Hanks balanced salt solution (HBSS) + 1 ml FBS). The cells where afterwards used for up to two hours stored at room temperature and after usage disposed due to unsterile environment at the microscope.

## 2.3. Microscopy

The used setup for the imaging is based on a Zeiss Axiovert 200 inverted microscope. The images where all taken in brightfield mode with the light source illuminating the sample from above coupled with a condenser and no optical filters. A 10x objective from Olympus (UPlanFL N 10x/0.3) was used in the microscope and it was coupled with an EM-CCD camera (Andor iXon DU-897D) for picturing. The software and hardware control were done with FEI Live Acquisition.

# 3. Results

## 3.1. Development of a Contact angle measurement set-up

To ensure that the produced PDMS chip bonds in a good and irreversible fashion with the glass slide the PDMS surface must be plasma activated. The surface energy of the activated surface can be measured by means of the water contact angle.

To image this contact angle (CA) between water and the PDMS surface, we assembled our own CA measurement set-up, consisting of a microscope stage (moveable in x and y direction) and a digital USB microscope (moveable in z direction and angle in x direction orientable) with adjustable magnification (50 – 1000X). The microscope was aligned horizontally with the stage to record the water drop from the side.

To measure the CA, the sample was placed onto the sample holder (glass slide) on the microscope stage. A 2 µl water drop was pipetted carefully onto the surface. After a short adjusting time of 10s the picture of the waterdrop was taken.

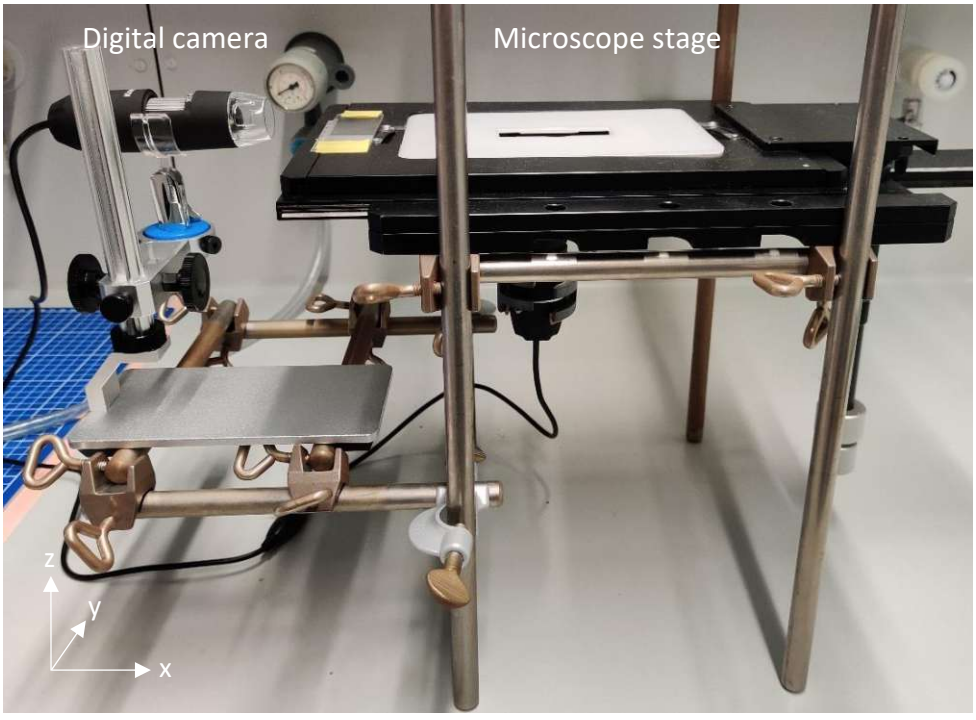


*Figure 12 Picture of the contact angle recording frame.*

The contact angle measurement was done using the low bond axisymmetric drop shape analysis (LBADSA) that is used as a plug-in for the ImageJ software. The analysis tool was

developed by Stalder et al. and is based on the fitting of the Young-Laplace equation to the image data. [16]

For the analysis the picture was loaded into ImageJ and was then converted into an 8-bit format. After opening the Drop analysis - LB-ADSA plug-in, a canvas overlay appears (see Figure 13). This canvas was then adjusted to fit to the outline of the waterdrop by adjusting the sliders of the plug-in window and the contact angle could then be read off.

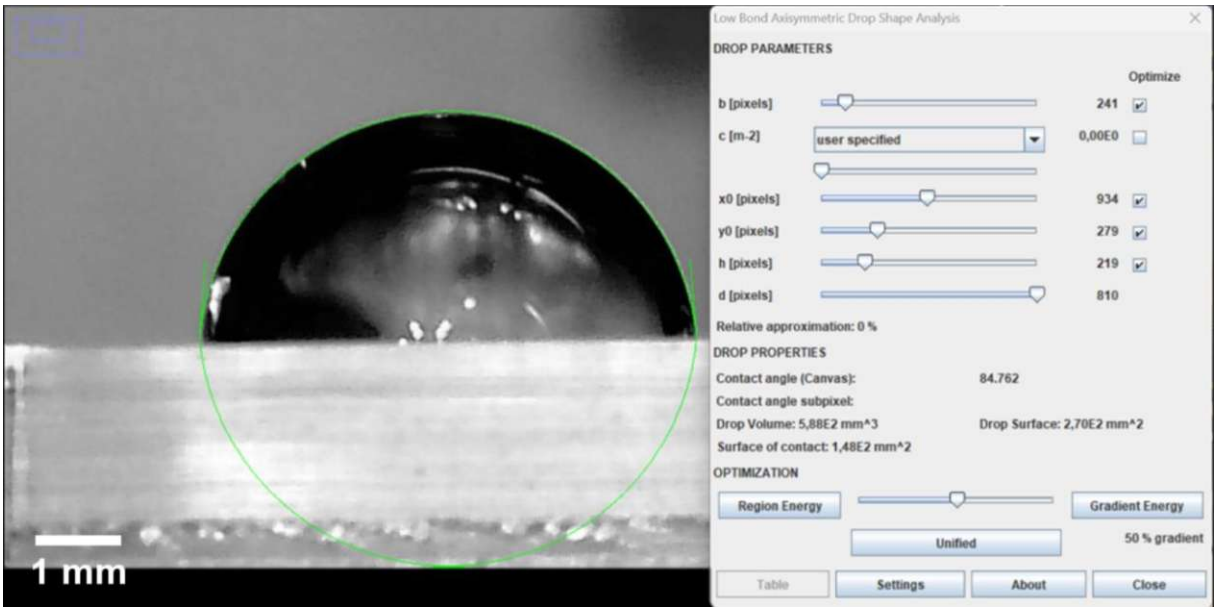


*Figure 13 Screenshot of the LB-ADSA plug-in window on the right side and the picture of the waterdrop which is analysed on the left side. The canvas (green line) is fitted to the waterdrop shape by using the sliders, afterwards the contact angle can be read.*

## 3.2. Plasma process stabilisation

To test the contact angle of the PDMS surface after activation with the plasma cleaner a PDMS layer of 2-3mm thickness was produced and then small rectangular pieces (side length between 5 to 10mm) were cut out. Three to five pieces were placed inside of the chamber at the back, near to the vacuum pump outlet. The PDMS pieces were plasma treated for 60 seconds with a power output of 10,2 W (medium setting) or 29,6 W (high setting) and stored in between measurements at room temperature (RT) inside a closed petri dish[17]. The contact angle was measured afterwards at different time points with the method described in 3.1.

During the first test runs the plasma treated test samples showed high fluctuations in the measured contact angle. As the PDMS surfaces activation depends on different parameters

as plasma chamber pressure, power output, process gas flow rates and exposure time during the plasma treatment[17], some of these parameters were tried to be stabilized or monitored.

### 3.2.1. Pressure and air flow

As the pressure could not be varied directly at the Harrick plasma cleaner it was extended with a vacuum gauge (Festo 537 810) on the three-way-valve to monitor the pressure inside. Plasma ignition in the plasma chamber was observed at a chamber pressures between 6600 and 8000 Pascal (Harrick Plasma cleaner manual recommends a pressure of around 80 Pa[17]). However, depending on the position of the three-way valve and how much the built-in needle valve was tightened, this value could change. Furthermore, we observed that the minimum reachable pressure increased after a few runs. This was also observed by changing plasma colours between runs. Hence, we concluded that our plasma process was quite unstable.

To stabilize the plasma process by controlling the air flow rate into the chamber, an air flow meter (Key Instruments MR3000 Air Flow Meter, 0,1 l/min. → 1,2 l/min.) was added. However, it was found that even at the lowest setting of the air flow meter, the pressure increased too much for effective plasma generation. We concluded that the used plasma cleaner has a very tight operation window, within which we cannot stabilize the process of plasma generation any further, given the available hardware components. Hence, we went on by standardizing our sample preparation for plasma activation instead.

### 3.2.2. Specimen location inside the plasma chamber

To ensure a good and reproducible quality of the treated PDMS parts, the influence of the placement of the pieces inside the plasma chamber was also looked at. The results (Figure 14) show that the parts should be placed as close as possible to the vacuum pump outlet (back of the plasma chamber) to reach the best activation, as the measured contact angle was smallest there. Possible explanation for this trend is the higher concentration of air close to the door of the reaction chamber due to inadequate sealing which impacts the quality and therefore the energy of the produced oxygen plasma.

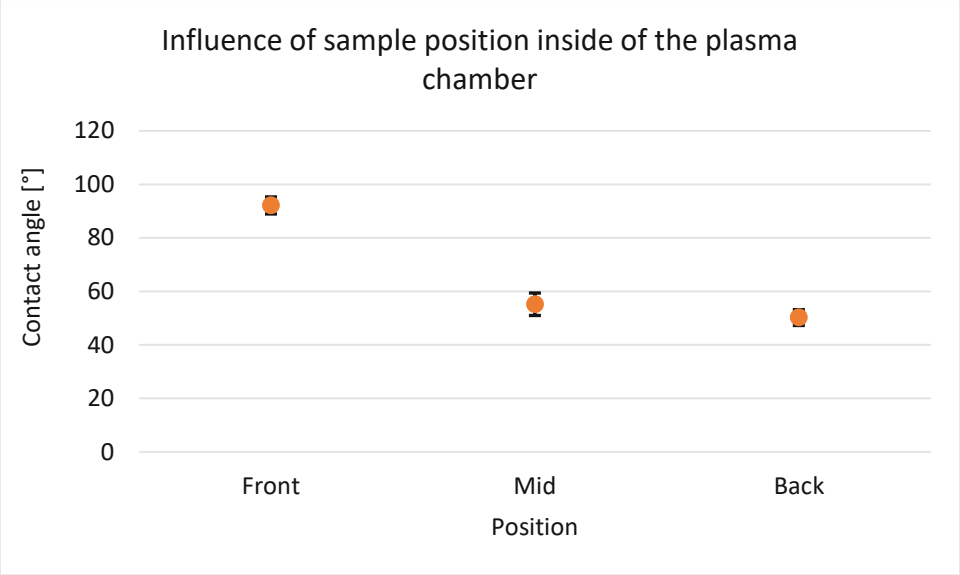


*Figure 14 The positioning of the treated pieces has a high impact on the result. Samples closer to the door (front) had a considerably higher contact angle after treatment compared to the ones closer to the vacuum pump outlet (back). The PDMS pieces were treated for 30s at 10,2W. For each position three PDMS pieces were plasma treated and then the mean contact angle was calculated. The error bars depict the standard deviation.*

## 3.3. PDMS-Glass bonding

According to Bhattacharya et al., from 2005, a contact angle below 5 degree corresponds to a good bonding strength between glass and PDMS and thus this CA was tried to be reached during the plasma activation process[5].

The first runs were done with an exposure time of 60s and a power output of 10,2W with measuring time points right after activation (0h) up to 4 hours after activation (Figure 15). The results showed that the contact angle of the PDMS directly after activation was around 41° which proved to be too high for bonding with a glass slide. We tracked the recovery of the PDMS' CA over the course of 4 hours and recorded an asymptotic curve that aligns well with data in the literature[18,19,20]. However, to reach the afore mentioned 5° CA threshold, a higher plasma power output was tried.

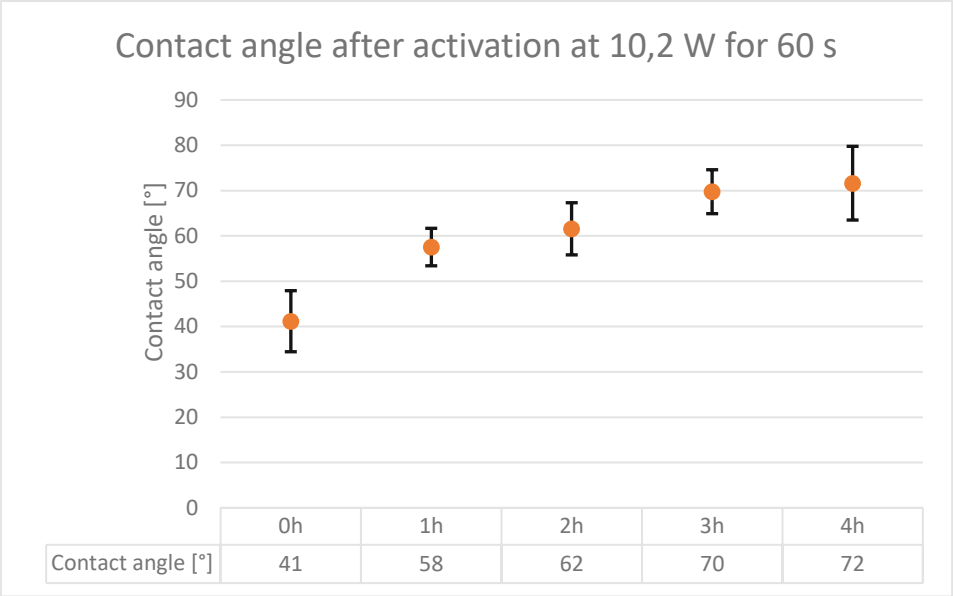


*Figure 15 Contact angle of PDMS treated for 60s with a power output of 10,2W. The experiment was done twice, with 25 PDMS pieces per run (5 pieces for each time point) and the depicted results represent the mean value with the standard deviation as error bars.*

The result of the runs with a higher power output of 29,6 W and exposure time of 60s showed a contact angle below the desired 5° to ensure a good bonding with a glass slide (Figure 16). The produced PDMS-Glass chips bonding strength was tested by carefully trying to separate them by hand directly after bonding. Although a good PDMS-glass bonding strength was given for most of the chips, some individual pieces showed partial delamination of PDMS from the glass. The exact reason for these fluctuations even after optimisation of the activation process could not be determined.

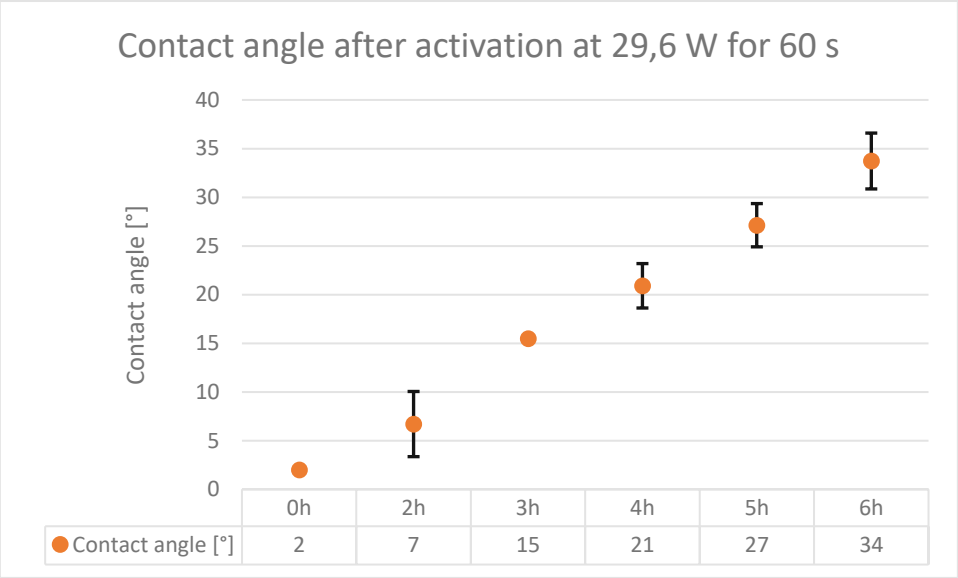


*Figure 16 Contact angle of PDMS treated for 60s at 29,6W. For each timepoint five PDMS pieces were plasma treated and the mean value was then used for the graph (Error bars depict the standard deviation)*

We also recorded the hydrophobic recovery after the activation process with higher power. The data show the typical regeneration of the hydrophobicity over time which is mainly due to the migration of low-molecular-weight PDMS chains from the bulk of the specimen to the surface. Additional effects that contribute to the rise in CA, are the reorientation of the polar groups from the surface to the bulk and condensation of the hydroxyl groups[18,19,20].

After the right parameters for the PDMS-glass bonding were found the next step was to look at the filling behaviour of the assembled SELTRAP chips.

## 3.4.Chip filling

To observe how the SELTRAP chip fills up, Imaging buffer (50 ml Hanks balanced salt solution (HBSS) + 1 ml FBS) was used. Directly after the activation and bonding around 25 µl of Imaging buffer (IB) was pipetted into the inlet port and the filing was imaged by using the setup described in 2.2 with brightfield imaging.

Due to the high hydrophilicity of the PDMS surface right after activation, the chips filled with a high velocity. The design at the inlet directs the liquid through increasingly narrow channels to the traps, then after passing them reaching the capillary pump (filling can be seen in Figure 17) at the end where the velocity of the flow stabilizes due to the prevalent capillary pressure.

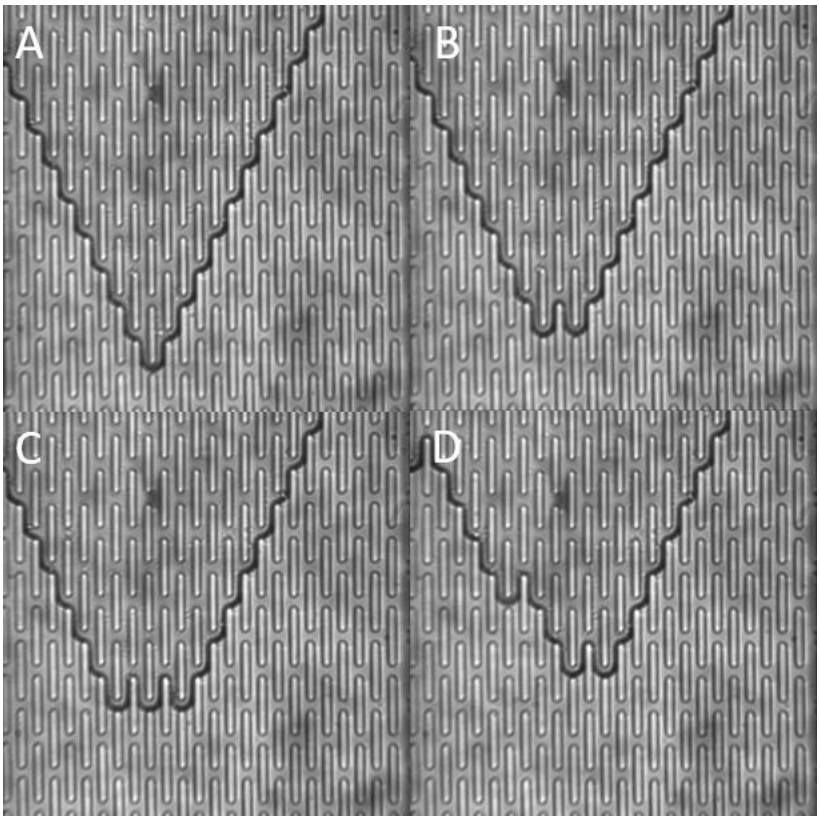


*Figure 17 Filling of the capillary pump. The pictures show how the filling front flows from pillar to pillar without entrapping air. A → B → C → D (time series).*

## 3.5. Validation of the traps with beads

To validate the particle trapping efficiency of the chip a polystyrene (PS) bead suspension with a concentration of 2000 beads/µl in ultra-pure water was used (Polybead® Black Dyed Microspheres 10.00µm from Polysciences).

The first test runs showed that the PS beads tended to clump together where the channel narrows down to 20µm and also in the curves of the flow channel. To prevent this effect, a final concentration of 2% Tween 20 (Sigma-Aldrich), which is a non-ionic detergent, was added to the solution to coat the PS beads and prevent agglomeration in our polar test solution. This was based on the paper from Gossett and Di Carlo in 2009 where they added 0,1% Tween 80 to prevent clumping[21]. The higher concentration of Tween 20 needed to achieve the same effect as Tween 80 is probably due to the more hydrophilic properties of Tween 20.

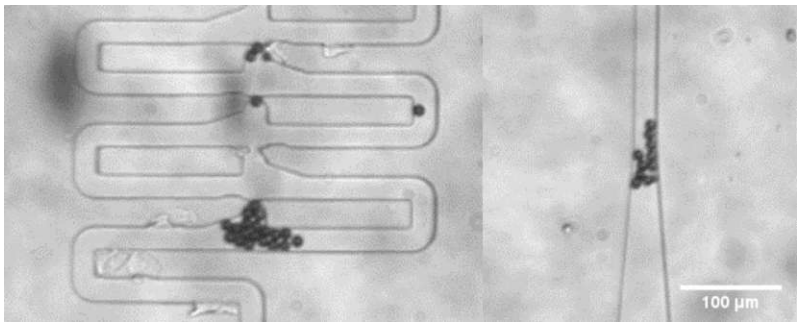


*Figure 18 Bead clumps formed preferably where the flow channel reached its narrowest width (right) or in the first trap (left).*

After the detergent was added the clumping behaviour of the beads decreased drastically but they still had a tendency of sticking to the hydrophilic channel walls (Figure 18). The tests with the adapted suspension solution showed that the traps fulfilled their function, but not all traps were filled. In all tests with freshly bonded chips (CA < 5°), only about ~10% (±2,5%) (the percentage was calculated by counting the number of filled traps in Figure 19 & Figure 20 and then dividing it by the total number of traps in the chip) of the traps were occupied with beads.

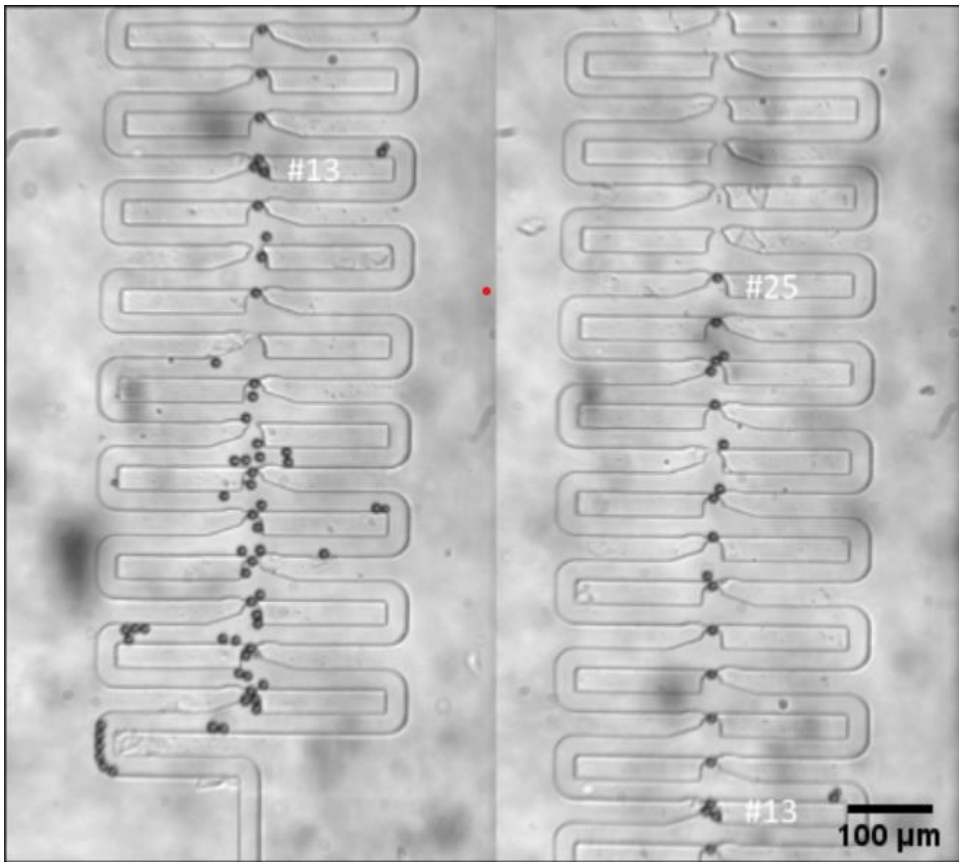


*Figure 19 The 1.1-200 design of the SELTRAP chip showed a maximum filling up to the 25th trap (number of traps labelled in the picture). Additionally, it can be seen how the beads tend to stick to the wall (curve before the first trap in the left picture) and even with added detergent sometimes clump together and block the flow channel.*

The 1.1-200, 1.11s-50 and 1.2-80 designs showed that the traps were filled with one and sometimes also with up to three beads. In the 1.1-200 chip (Figure 19) design the sticking of the beads to the wall and the clumping can be seen. In the 1.11s-50 and 1.2-80 designs, it was observed that the beads occasionally (when and why exactly could not be determined) passed through the trapping channel due to the high capillary pressure in the chip.

The 1.0-200 design could not be evaluated because the chip could not be filled in any test. This was either due to bonding errors of the whole chip, or in the cases where the chip was successfully bonded and filled with the suspension, the beads got stuck right after the inlet port and thus did not reach the traps. However, the filling behaviour and the trapping efficiency is expected to be like that of design 1.1-200 as the trap design is the same and only the relative position of the traps is different.

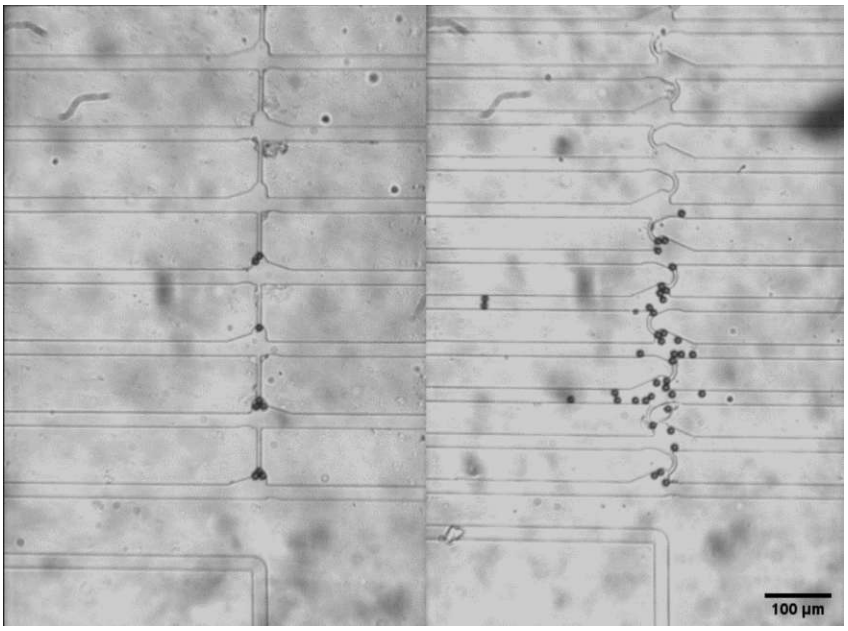


*Figure 20 Left: Trapping efficiency of the 1.11s-50 chip design. Only a small number of beads reached the trapping area and the traps tended to be filled with more than one bead. Right: In the 1.2-80 design the beads had a tendency to get stuck to the walls around the traps, probably due to the different pressure profile around the trap compared to the other designs (see 1.3.2).*

## 3.6. Filling of the chips with cells

After the effectivity of the traps was confirmed, the next step was to try catching murine T-cells. The average width of these cells measures around 7 µm (measured from different pictures with ImageJ) thus trapping should be possible. To prepare the cells for the experiments 100 – 200 µl of the cell suspension was centrifuged, the T-cell media was removed, and the cells were then resuspended in an equal amount of Imaging buffer. The cell concentration was not determined as the number of cells is not a decisive factor for the experiments.

For the first filling tests the chips were used right after activation (CA < 5°) and thus still expressed a high capillary pressure. Although this causes the chip to fill in short time, it had the side effect that the cells were pushed through the traps at high speed, as they are deformable, unlike the rigid beads. The passing through the trapping channel could also be seen with the beads but in a much lower frequency compared to the live cells.

As an alternative to the mouse T-cells, the chip was then tested with Jurkat T cells (average size 11.5 µm[22]). Although the cells are bigger in size, the same behaviour as with the mouse T-cells was observed as the cells were also pushed through the traps (Figure 21).

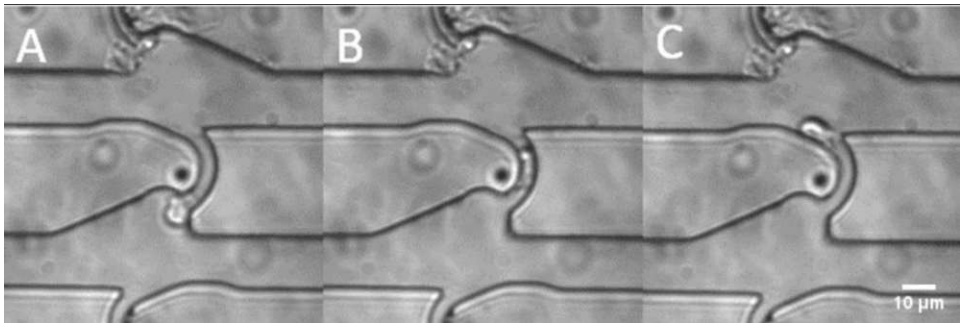


*Figure 21 Timeseries from A → B → C of how a Jurkat T cell squeezes through the trapping channel. The cell passed the trap in about 600 ms (cycle time of 200 ms per picture)*

## 3.7. Lowering of the capillary pressure

To efficiently trap the cells the capillary pressure had to be lowered to ensure that the cells stay inside of the trap and do not pass through it. The idea was to raise the contact angle from the initial < 5° to a range between 45° and 55° degrees after activation as this roughly represents the range between hydrophilicity and total hydrophobicity (CA > 90°) and test runs with chips with a CA > 60° showed a very slow filling velocity (after 30 minutes the liquid only reached up to the first trap). The hydrophobic recovery rate of PDMS is not only affected by the effects described in 3.3 but also the storage conditions such as temperature and humidity play a role[20].

To achieve the desired contact angle (~50°) by just letting the chip rest at RT after activation, the extrapolated data from Figure 16 shows that the waiting time lies in between 7,75 and 9,30 hours. This long rest period would be very impractical for a normal lab day.

In the paper by Bacharouche et al. from 2013 the authors tested how the hydrophobic recovery rate of PDMS behaves after argon plasma treatment (treatment time 60s at 60W) under the influence of different temperature storing conditions. Their data showed that the contact angle of the PDMS stored at 4°C is around ~50° 24 hours after activation and reaches a plateau. This effect could be used create an increased time window in which the chips' CA

stay within a desired range and were the SELTRAP chips could be used for cell trapping experiments. [23]

Hence we tried to reproduce these results without the use of a argon plasma cleaner. Because of the lower power output of our device compared to the one mentioned in the literature (Bacharouche et al.), the treatment time was increased to 120 s. However, the experiments did not give the desired results as the contact angle mean value of the treated PDMS pieces (6 pieces were tested for each time point) was around 67° after 24 h storage at 4°C (test samples were stored in a fridge inside a dessicator filled with silica beads to control humidity) and reached 79° after 72 h (~70° after 72 h in the above mentioned paper). We could therefore not reach the desired CA plateu (see Figure 22 for results).

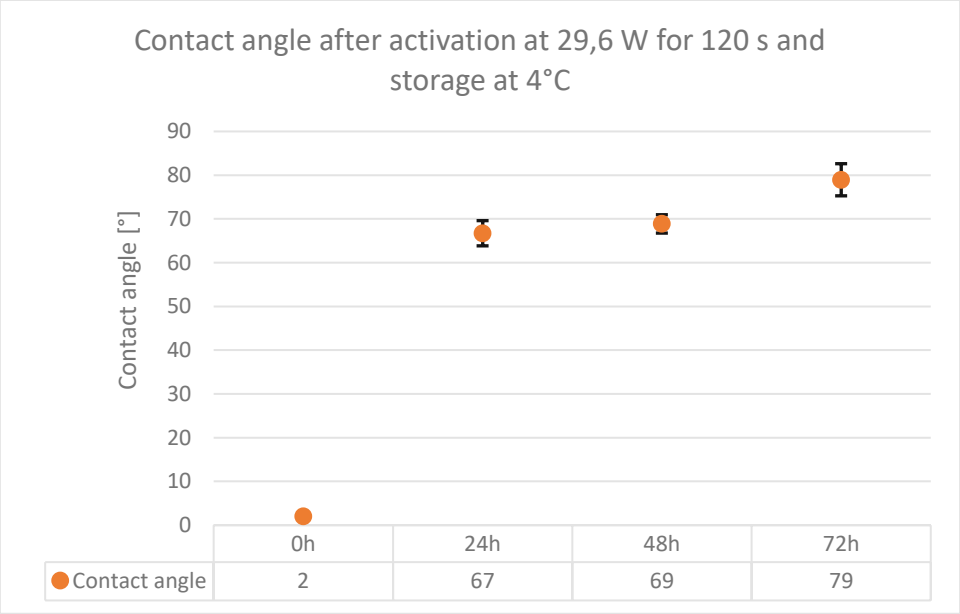


*Figure 22 Hydrophobic recovery of PDMS treated for 120 s at 29,6 W and then stored at 4°C. For each timepoint 6 pieces were plasma treated and then the CA was measured (error bars represent the standard deviation).*

As the contact angle was too high after 24 hours, this approach to reduce the capillary pressure was not pursued further. However, the temperature aspect led to a new approach for a series of experiments which consisted of conditioning the chips in an oven over a set amount of time. The idea behind this approach would be to raise the diffusion coefficient of the low-molecular-weigth PDMS oligomeres which rise from the bulk to the surface as this would lead to a higher hydrophobic recovery rate.So instead of decreasing the kinetics to

increase the time window in wich the chips have a desired CA we tried to accelerate the CA recovery after plasma bonding to use our chips shortly after production.

The first attempts indicated that a conditioning time of 30 minutes at 40°C (Plasma treatment 60 s at 29,6 W) gives the desired CA of around 50° (Figure 23). However, the filling tests showed that the chip is difficult to fill and quite prominent fluctuations in the filling speed between inlet, trap and just before the capillary pump occurred. This can mainly be attributed to local aging differences in the chip which occur during the heating process. The parts of the chip which are directly exposed to the hot air stream (inlet) tend to age faster than the trapping area, where only heat conduction and not convection occurs.

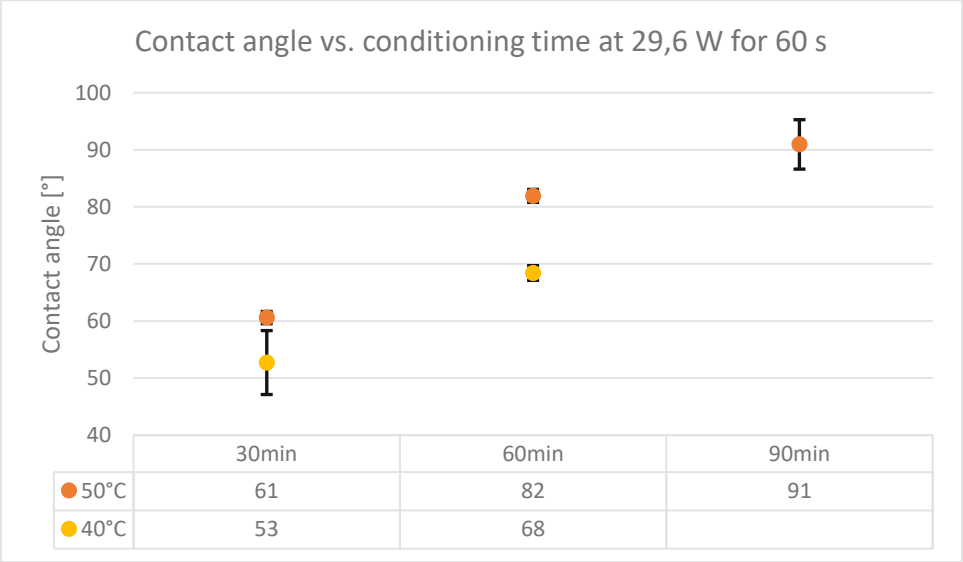


*Figure 23 Contact angle versus conditioning time at different temperatures (40°C yellow data set and 50°C orange data set). For each time point at both temperatures three PDMS pieces were plasma treated and the mean value was calculated (error bard represent the standard deviation of each time point).*

To countermeasure these phenomena different approaches were tried. A longer activation time of 180 s at 29,6 W showed that the fluctuations in filling time were reduced but this led to an increase in the conditioning temperature to 50°C to get the desired contact angle in a range of about 50° after 30 minutes of treatment. Another measure was to seal the inlet and outlet ports with tape during oven treatment and subsequent second activation in the plasma chamber of the chip (without tape) for 30s at 29,6 W to increase the hydrophilicity of the inlet port and to countereffect the low initial filling velocity of the chip. The average contact angle after the measures was 51° (Figure 24 shows the measurement series) and the filling

behaviour improved compared to the initial conditioning conditions at 40°C with 60 s activation.

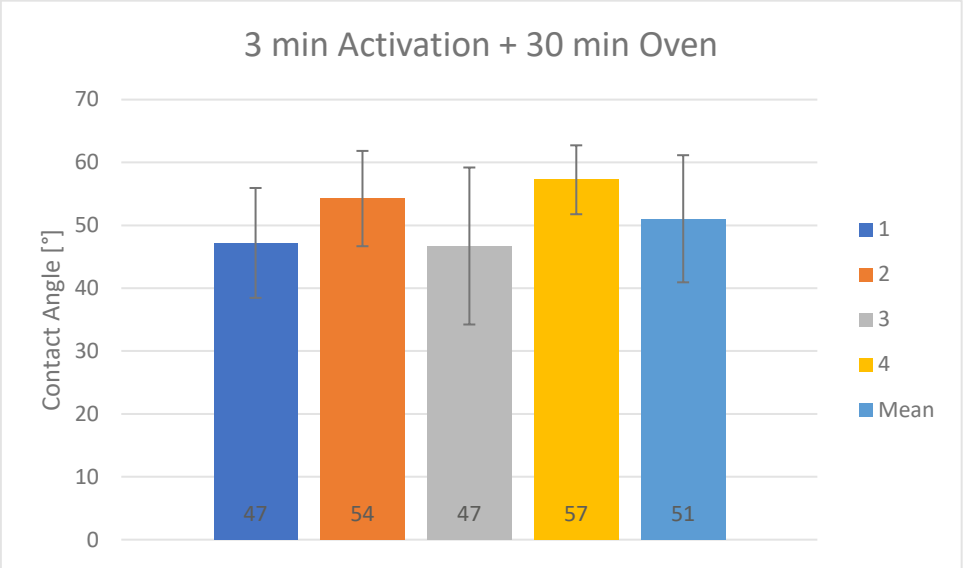


*Figure 24 Data from 4 series of measurements under identical conditions (180s activation at 29.6W, 30 minutes at 50°C in the oven, 4 to 5 samples per series of measurements, error bars are the standard deviation). Samples were conditioned in the oven in a Petri dish with the lid half open to avoid direct contact with circulating air. Bar on the far right shows the overall average over all samples.*

## 3.8. Filling of the conditioned chip

The filling behaviour of the conditioned chips was tested again with the bead suspension which was used in 3.5. The test runs were conducted with the designs 1.1-200, 1-11s-50 and 1.2-80, the 1.0-200 was not tested due to the -described problems in 3.5. The conditioned chips filled significantly slower than the freshly bonded ones due to the lower capillary pressure, but the effectiveness of the traps remained. However, in general, a lower number of traps filled compared to the unconditioned chips. In addition, it has been observed that more than one bead is found in the traps, probably due to the reduced flow velocity, which makes them more likely to come into contact around the traps and clump together.

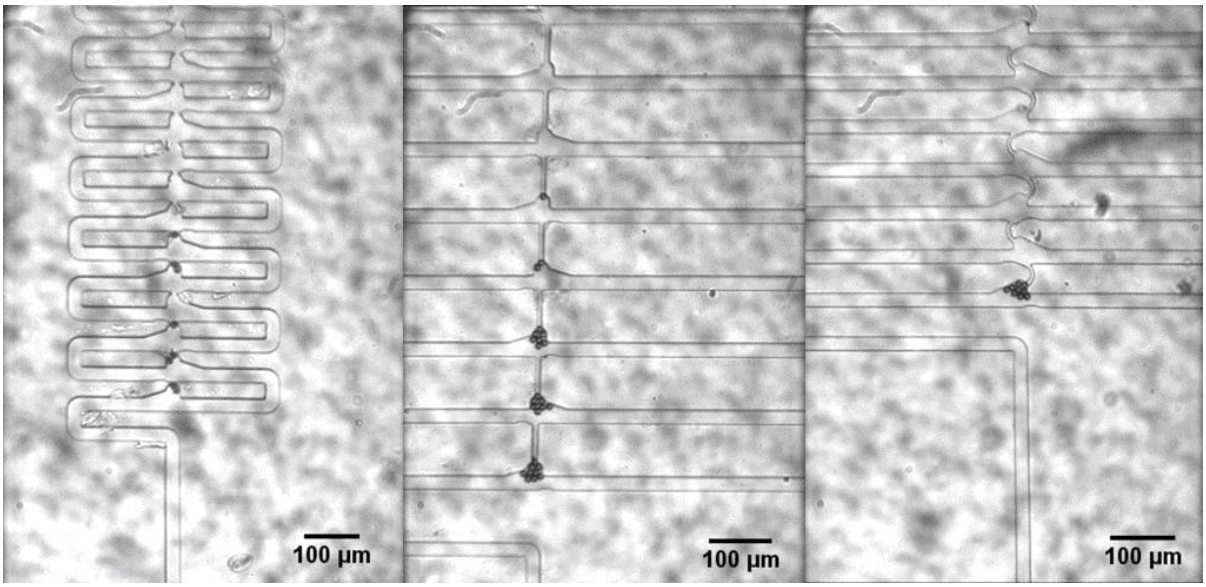


*Figure 25 From left to right Design 1.1-200, 1-11s-50 and 1.2-80. The last design failed to trap the beads in more than one trap, every bead which made it to the trapping channel clumped together in the first trap. This clumping can also be observed in the 1.11s-50 design. The 1.1-200 chip trapped a significantly lower number of beads compared to the unconditioned chips.*

After the validation with the beads was done, the next step was to fill the chip again with Jurkat T cells. The tests showed the efficiency of the traps in the 1.1-200 and the 1.2-80 design and in contrast to the experiments with the beads, more traps were filled with cells in the two designs. Figure 25 shows that the 1.1-200 design could be filled up to the 14th trap and 1.2-80 up to the 8th trap, which corresponds to an occupancy of 7% and 10% of the traps with cells, respectively. Although the 1.11s-50 design filled with liquid in the experiments, the cells were stuck in every try at the inlet and did not reach the traps.

Although the capillary pressure is reduced in the conditioned chips, some cells were still observed to be pushed through the trapping channel in the 1.2-80 design. This is probably due to the higher flow velocity in the smaller trapping channel. This behaviour was rarely observed in the 1.1-200 design (Figure 26 shows the differences).

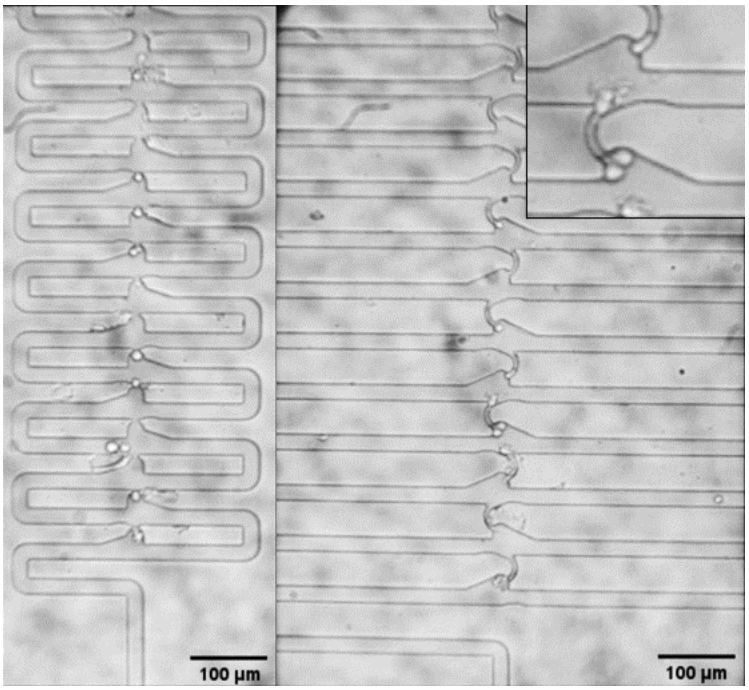


*Figure 26 Trapping efficiency of the conditioned SELTRAP chips. On the left the 1.1-200 design is filled up to the 14th trap with cells and the 1.2-80 on the right up to the 8th trap. In the right upper corner, a cut-out of the 4th and 5th trap is shown where the cells can be seen how they are pushed into the trapping channel.*

In general, the SELTRAP-chip fulfils its purpose of its self-filling and cell trapping capabilities but with restrictions regarding the number of occupied traps.

## 3.9. Bonding errors and wear out

After around 40+ usages of the SU-8 wafer, the chips have started to show more and more signs of wear. The most observed phenomenon was mis-bonding at the inlet of the chip (can be seen in Figure 27 A), where the top side bonded with the glass and the flow channels were (partially) closed as a result. This made the filling of the chip no longer possible or, if a small part of the channel was still available, the filling speed was very slow (similar to chips with a CA > 60°).

Other commonly seen signs of wear are pictured in Figure 27 B&C (B: 1.1-200, C: 1.11s-50). The 1.1-200 design showed a clear loss of shape which was accompanied by a loss of function of the traps. And with the 1.11s-50 design, it could be observed that the trapping channel was no longer correctly moulded in some traps.

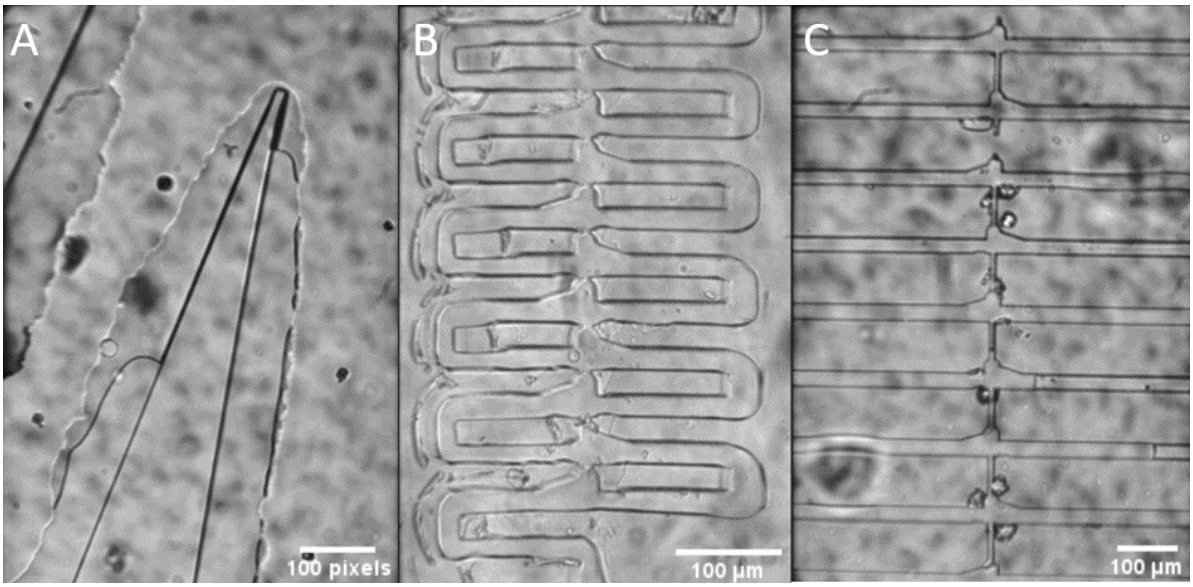


*Figure 27 A shows the undesired bonding of the top surface of the inlet with the glass which leads to a loss of function of the chip. B & C show how wafer wear causes chips to lose shape and function over time.*

# 4. Discussion

## 4.1.Self-filling function

The self-filling function of the SELTRAP chip is one of its two main functions. The experiments carried out have shown that this function of the chip is fulfilled to the required extent and that the chosen design for the capillary pump meets the requirements (no air pockets and no clogging by particles) and further enables a constant flow rate as described in literature[13].

One problem which was observed in the chips was an unsteady filling velocity in the trapping area. This can mostly be attributed to an irregular plasma treatment of the PDMS surface inside of the plasma chamber which results in local CA differences and thus different capillary pressures along the flowing channel. This observation of the uneven plasma treatment could also partly explain the high standard deviation of the measured contact angles of the PDMS surface which in some measuring series was over 10° (samples were always placed at the same relative position in the chamber). We expect the unsteady filling behaviour to be solved by a more controlled plasma activation process. Our approaches to stabilize the plasma process with the used plasma cleaner did not yield reproducible results. Therefore, we recommend using a dedicated plasma chamber including precision pressure regulators, process gases (i.e., $O_2$) and a process timer.

## 4.2. Cell trapping ability and behaviour

During the course of the master thesis the cell trapping ability of the chip could be validated with the usage of cell-sized polystyrene beads and also with Jurkat T cells. However, it could be shown that by far not all traps could be filled with cells; the occupancy corresponded to about 7-10% (the percentage was calculated by counting the number of filled traps in Figure 26 and then dividing it by the total number of traps in the chip) in the conditioned chips, depending on the design. This low percentage of filled traps can be attributed to two main factors, (i) low flow velocity at the inlet which caused beads and cells to sediment inside the inlet port and (ii) the increase in flow resistance with increasing number of occupied traps. With increasing flow resistance, the flow rate decreases, hence it is even harder to guide new particles into the microchannel. These phenomena are directly linked to the design of the microchannels in the SELTRAP chip. Depending on the power of the capillary pump more or less traps can be occupied with particles. Moreover, interactions between the particles

and the SELTRAP chips internal surfaces were observed, which resulted in particle sticking to the channel walls before they reached the trap areas. Adding surfactant to the PS beads reduced the bead-bead interactions, beads-PDMS sticking could still not be fully excluded though. Cells sticking to the wall is an issue commonly observed in microfluidics. It is frequently addressed by incubation of PDMS channels with Pluronic additives[24]. Since our device relies on a single fill operation, preliminary coatings of the interior microchannel networks are not feasible.

## 4.3. Contact angle measurement

The method for contact angle measurement which was built during the master thesis is more cost efficient (highest cost item was the digital camera with a price of under 25€) compared to a standard optical tensiometer which is normally used to measure the CA. But due to its design it's also more prone for error susceptibility because the camera has to be manually adjusted to face the drop directly from upfront which can lead to deviations and the drop is manually applied onto the surface of the material which can also lead to errors (wrong handling of the pipette for example). Moreover, we did not control room temperature and humidity, which are also influencing the contact angle.

Another aspect of the contact angle measurements is that the obtained contact angle results were all measured on PDMS samples where the surface was probably not exposed to the same conditions as the channels inside the chip and thus the contact angles may differ. Still, the CA measurement device was a valuable tool to predict the efficiency of plasma activation and to tune the filling behaviour of the SELTRAP chips.

## 4.4. Parameters and design

The results of the different chip designs indicate that each has its own advantages and disadvantages. The 1.1-200 design had the greatest number of traps filled compared to the other two tested designs and the cells also did not show a deformation of their shape in the traps as it can be seen in the 1.2-80 chip (Figure 26 shows the difference (round shape for the 1.1-200 design and more elongated cells in the 1.2-80). The difference in trapping efficiency is probably due to the difference in the ratio of volumetric flow rates in the trapping and flowing channel (Q1/Q2 see formula II in 1.3.1) between the two designs. The ratio for the 1.1-200 design is 3.36 and only 1.67 for 1.2-80. The cell deformation seen in the traps of 1.2-80 chips

is likely a result of the higher maximal flow rates in the trapping areas, as predicted by our flow simulations.

The used parameters for the conditioning of the SELTRAP chip (Plasma activation for 3 minutes + 30 minutes in the oven + second plasma treatment for 30 seconds (both at 29,6W)) showed the best results when considering the trapping efficiency of the chip. The measured mean contact angle of the PDMS was after the treatment at 51° which was high enough for the chips to fill in a reasonable time without an excess number of cells which are squeezed through the traps due to a too high capillary pressure.

If the plasma treatment process could be stabilised with the points discussed in 4.1 the initial plasma activation time of three minutes could surely be reduced. The oven treatment time would have to be determined anew then.

## 4.5. Wear out

The observed wear out of the SU-8 master is unfortunately typical for soft lithography as the structures in the used photoresist are damaged when the cured PDMS is removed from it. This is also described in the review of Ansari et al. where they describe techniques for surface modification in PDMS-PDMS double casting. [25] This method could also be used in our case to prevent the downgrading of the original master by producing a PDMS master. The new master has then to be surface treated e.g., different chemical or non-chemical treatments described in the paper to prevent sticking of the newly casted PDMS to the PDMS master.

# 5. Conclusion and outlook

The obtained results for the SELTRAP chip indicate that the idea to produce an inexpensive and easy-to-use microfluidic chip for single cell trapping and microscopy is possible and feasible, but it also shows drawbacks in the design. To optimise the cell capture behaviour, fewer traps would have to be designed in series and the inflow channel from the inlet to the first trap has to be adapted to minimize the drop in capillary pressure. The base for a new design should be derived from the 1.1-200 chip as it showed the best trapping ability, and the cells retained their shape while being trapped.

A possible use of a newly designed chip could for example be to study the interaction of cells with coated beads, e.g., TCR-pMHC (T-cell receptor – peptide major histocompatibility complex) interactions[26]. By varying the flow speed inside of the channel, the binding kinetics between the TCR and pMHC molecules can be observed and estimated. Also, by using coated beads the used proteins can be interchanged relatively easy.

On the other hand, the change in cell shape which could be observed in the 1.2-80 chips, could be used to study mechanobiological changes of cells when they are squeezed. One possible use of these microfluidic constrictions of cells is a vector-free delivery of macromolecules into the cytosol. [27]

# References


1. Dietzel, A. Microsystems for pharmatechnology: Manipulation of fluids, particles, droplets, and cells. *Microsystems Pharmatechnology Manip. Fluids, Part. Droplets, Cells* 1–348 (2016) doi:10.1007/978-3-319-26920-7.
2. Whitesides, G. M. The origins and the future of microfluidics. *Nature* **442**, 368–373 (2006).
3. Squires, T. M. & Quake, S. R. Microfluidics: Fluid physics at the nanoliter scale. *Rev. Mod. Phys.* **77**, 977–1026 (2005).
4. Chen, J., Chen, D., Xie, Y., Yuan, T. & Chen, X. Progress of microfluidics for biology and medicine. *Nano-Micro Lett.* **5**, 66–80 (2013).
5. Bhattacharya, S., Datta, A., Berg, J. M. & Gangopadhyay, S. Studies on surface wettability of poly(dimethyl) siloxane (PDMS) and glass under oxygen-plasma treatment and correlation with bond strength. *J. Microelectromechanical Syst.* **14**, 590–597 (2005).
6. Raj M, K. & Chakraborty, S. PDMS microfluidics: A mini review. *J. Appl. Polym. Sci.* **137**, (2020).
7. HarrickPlasma. PDMS BONDING (MICROFLUIDICS). https://harrickplasma.com/pdms-bonding/.
8. Ren, K., Zhou, J. & Wu, H. Materials for microfluidic chip fabrication. *Acc. Chem. Res.* **46**, 2396–2406 (2013).
9. Nilsson, J., Evander, M., Hammarström, B. & Laurell, T. Review of cell and particle trapping in microfluidic systems. *Anal. Chim. Acta* **649**, 141–157 (2009).
10. Yin, H. & Marshall, D. Microfluidics for single cell analysis. *Curr. Opin. Biotechnol.* **23**, 110–119 (2012).
11. Tan, W. H. & Takeuchi, S. A trap-and-release integrated microfluidic system for dynamic microarray applications. *Proc. Natl. Acad. Sci. U. S. A.* **104**, 1146–1151 (2007).
12. Kimmerling, R. J. *et al.* A microfluidic platform enabling single-cell RNA-seq of multigenerational lineages. *Nat. Commun.* **7**, 1–7 (2016).
13. Zimmermann, M., Schmid, H., Hunziker, P. & Delamarche, E. Capillary pumps for autonomous capillary systems. *Lab Chip* **7**, 119–125 (2007).
14. Brighton Science. What is Contact Angle? https://www.brighton-science.com/what-is-contact-angle.
15. Kim, P. *et al.* Soft lithography for microfluidics: A Review. *Biochip J.* **2**, 1–11 (2008).
16. Stalder, A. F. *et al.* Low-bond axisymmetric drop shape analysis for surface tension and contact angle measurements of sessile drops. *Colloids Surfaces A Physicochem. Eng. Asp.* **364**, 72–81 (2010).
17. HarrickPlasma. User Manual Harrick Plasma Cleaner. https://labs.jhu.edu/wp-content/uploads/2016/04/Harrick-Plasma-Cleaner-Users-Manual.pdf.

18. Fritz, J. L. & Owen, M. J. Hydrophobic recovery of plasma-treated polydimethylsiloxane. *J. Adhes.* **54**, 33–45 (1995).

19. Eddington, D. T., Puccinelli, J. P. & Beebe, D. J. Thermal aging and reduced hydrophobic recovery of polydimethylsiloxane. *Sensors Actuators, B Chem.* **114**, 170–172 (2006).

20. Tan, S. H., Nguyen, N. T., Chua, Y. C. & Kang, T. G. Oxygen plasma treatment for reducing hydrophobicity of a sealed polydimethylsiloxane microchannel. *Biomicrofluidics* **4**, 1–8 (2010).

21. Gossett, D. R. & Di Carlo, D. Particle focusing mechanisms in curving confined flows. *Anal. Chem.* **81**, 8459–8465 (2009).

22. Rosenbluth, M. J., Lam, W. A. & Fletcher, D. A. Force microscopy of nonadherent cells: A comparison of leukemia cell deformability. *Biophys. J.* **90**, 2994–3003 (2006).

23. Bacharouche, J., Haidara, H., Kunemann, P., Vallat, M. F. & Roucoules, V. Singularities in hydrophobic recovery of plasma treated polydimethylsiloxane surfaces under non-contaminant atmosphere. *Sensors Actuators, A Phys.* **197**, 25–29 (2013).

24. Luk, V. N., Mo, G. C. & Wheeler, A. R. Pluronic Additives: A Solution to Sticky Problems in Digital Microfluidics. doi:10.1021/la7039509.

25. Ansari, A., Trehan, R., Watson, C. & Senyo, S. Increasing silicone mold longevity: a review of surface modification techniques for PDMS-PDMS double casting. *Soft Mater.* **19**, 388–399 (2021).

26. Stockslager, M. A. *et al.* Microfluidic platform for characterizing TCR-pMHC interactions. *Biomicrofluidics* **11**, (2017).

27. Sharei, A. *et al.* A vector-free microfluidic platform for intracellular delivery. *Proc. Natl. Acad. Sci. U. S. A.* **110**, 2082–2087 (2013).